672 *J. Chem. Eng. Data* **2000,** *45,* 672−677

Solubility of Triphenylphosphine, Tris(*p*-fluorophenyl)phosphine, Tris(pentafluorophenyl)phosphine, and Tris(*p*-trifluoromethylphenyl)phosphine in Liquid and Supercritical Carbon Dioxide

Klaus-D. Wagner, Nicolaus Dahmen,* and Eckhard Dinjus

Institut für Technische Chemie CPV, Forschungszentrum Karlsruhe, D-76021 Karlsruhe, Germany

The solubility of the solid substances triphenylphosphine $P(C_6H_5)_3$, tris(*p*-fluorophenyl)phosphine $P(C_6H_4F)_3$, tris(pentafluorophenyl)phosphine $P(C_6F_5)_3$, and tris(*p*-trifluoromethylphenyl)phosphine $P[4-(CF_3)C_6H_4]_3$ in CO_2 was measured as a function of pressure at 300.0 K, 310.0 K, 320.0 K, and, in the case of triphenylphosphine, at 330.0 K. For this purpose, a new recirculation view cell apparatus coupled to a high-performance liquid chromatograph was constructed. The solubility *S* of triphenylphosphine was measured up to 30.3 MPa and up to a maximum of 0.119 mol/L, tris(pentafluorophenyl)phosphine up to 12.0 MPa and 0.246 mol/L, tris(*p*-fluorophenyl)phosphine up to 18.9 MPa and 0.468 mol/L, and tris(*p*-trifluoromethylphenyl)phosphine up to 12.0 MPa and 0.470 mol/L. The increasing degree of fluorination in these four substances led to an increase of their solubility in carbon dioxide.

Introduction

In the context of extraction of metal chelates from the aqueous environment with supercritical carbon dioxide, much work has been done on the solubility of ligands and metal−ligand complexes (Ashraf-Khorassani et al., 1997a; Wai and Wang, 1997; Smart et al., 1997). However, few measurements have been made on the solubilities of ligands and metal species taking part in the chemical reactions (Kainz et al., 1997; Kreher et al., 1998; Stradi et al., 1998). As the catalyst in some reactions is formed in situ, the solubilities of the pure ligands as well as of the whole complexes are of interest for reactions in supercritical carbon dioxide. Phosphines play an important role as ligands of catalysts in reactions carried out not only in conventional solvents but also in supercritical carbon dioxide. The perfluorinated triphenylphosphine $P(C_6F_5)_3$ and $P[3,5-(CF_3)_2C_6H_3]_3$ were used by Morita et al. (1998) for a carbon−carbon bond coupling reaction. Palo and Erkey (1998) tested $P[4-(CF_3)C_6H_4]_3$ as a ligand in a rhodium catalyst for the hydroformylation of 1-octene with success. Despite the increasing interest in the solubilities of those ligands in CO_2, we found only data for triphenylphosphine, trioctylphosphine, and didodecylphosphine in the comprehensive publication of Schmitt and Reid (1988). It is known that fluorination of the solutes enhances the solubility in CO_2 drastically. In the case of fluorinated alcohols, Yee et al. (1992) concluded the higher solubility in carbon dioxide to be primarily the result of weaker hydrogen-bonding energies. Furthermore, the repulsive nature of the fluorine atoms decreases the solute−solute interactions and improves the solubility in a fluid with low relative permittivity such as carbon dioxide. More often a specific interaction is assumed between the fluorine, rich with electrons, and the CO_2 with its lower electron density (Yazdi and Beckman, 1996). In NMR measurements the influence of temperature and density of CO_2 on the chemical shifts of ^1H and ^{13}F in fluorinated and nonfluorinated hydrocarbons were investigated (Dardin et al., 1998). The results suggest a specific interaction between the unlike molecules. IR investigations point at an electrostatic attraction between the CO_2 quadrupole and C−F dipole (Kazarian et al., 1996).

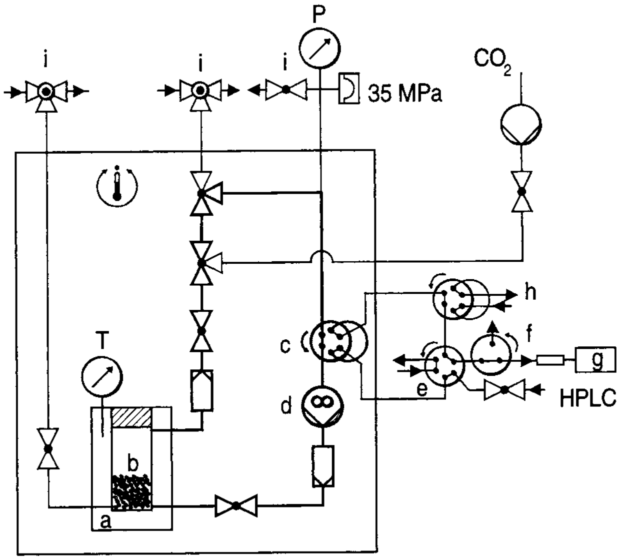

Figure 1. Schematic diagram of the experimental apparatus: a, high-pressure cell with sapphire window topside; b, solid substance; c, sampling valve; d, gear pump; e, switching valve between HPLC and cleaning with liquid CO_2; f, CO_2 outlet during sampling; g, HPLC detector; h, calibration valve; i, venting, cleaning, and drying lines.

In this work different commercially available phosphines were selected to study the effect of fluorination on phase equilibria. Depending on temperature and pressure, the solubility of even chemically similar ligands can show large differences in solubility. In view of homogeneous reactions catalyzed by organometallic substances, it makes a difference if the state of aggregation of a substance is solid or liquid, e.g., if in situ formation of catalysts is desired.

10.1021/je9902995 CCC: $19.00

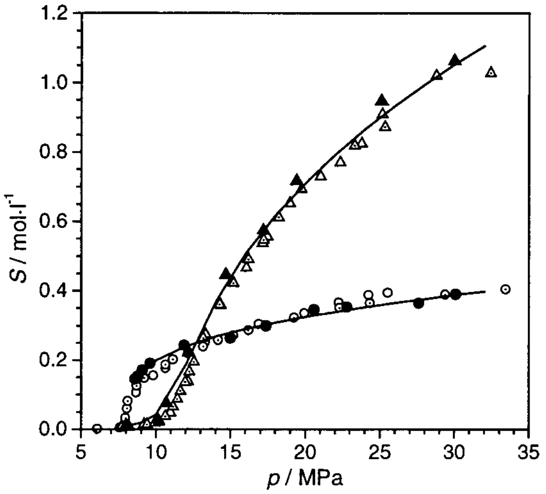

Figure 2. Solubility of naphthalene in carbon dioxide: this work, (●) 308 K, (▲) 328 K; open symbols, data from McHugh and Paulaitis (1980); dot centered symbols, data from Tsekhanskaya et al. (1964). Interpolations are from eq 1 of this work.

Because of these reasons, knowledge of the complete phase diagrams as a function of temperature and pressure is desirable to decide whether or not a substance is suitable for a reaction in supercritical carbon dioxide.

In the experimental range investigated here, phase equilibrium phenomena were expected which are commonly found in CO_2 systems containing substances of low volatility, e.g., melting, liquid−liquid equilibria, and three-phase equilibria (McHugh and Krukonis, 1986; Peters, 1994; Peters et al., 1995; Luks and Kohn, 1984).

Experimental Section

Materials. Triphenylphosphine (mp 353 K) was supplied by Merck with a purity higher than 99%, tris(pentafluorophenyl)phosphine (mp 381−383 K) by Aldrich (>97%), tris(*p*-fluorophenyl)phosphine (mp 352−353 K) by Strem Chemicals (>99%), tris(*p*-trifluoromethylphenyl)phosphine (mp 346−348 K) by Strem (>97%), and naphthalene by Merck. Carbon dioxide was supplied by Messer Griesheim with a purity better than 99.995%. The substances were used without further purification.

Apparatus. To measure the solubility of the solid substances, which are only available in small amounts, a new apparatus with a 10 mL view cell was constructed (Figure 1). The solid material is filled in via a sapphire window (SITEC, 12 mm i.d.) topside of the autoclave (a). Through the window, the entire volume of the autoclave is observed via a CCD camera connected to an endoscope with light beam. So the existence of a second phase as well as the state of aggregation of this phase can be detected. Carbon dioxide is compressed into the cell by a pneumatic pump (Pickel PM 101) up to the desired pressure. To prevent precipitation of solid material in the capillary tubes, the pressure is only increased during a series of measurements. The entire apparatus is placed in an oil bath (Haake Sil 110) which is kept at the desired temperature ±0.1 K by a thermostat (Haake N6). To equilibrate the system, the fluid phase is recirculated by a gear pump (d) (Micropumps 1805C). Approximately 10 min after the filling with carbon dioxide, when the pressure remains constant, 5 min of recirculation was found to be enough to attain equilibrium. The pressure transducer (WIKA type 891.23.510, wire strain gauge, maximum pressure 60 MPa) was calibrated by a pressure balance (Haenni & Cie m.b.H.) at ambient temperature. To avoid a temperature compensation, the pressure transducer is placed outside the liquid bath and is connected to the apparatus via a 20 cm long tube ($^1/_{16}$ in. i.d.). The pressure transducer is accurate to ±0.1 MPa. Temperature is measured by a PT-100 resistance thermometer in the wall of the cell with an uncertainty of ±0.1 K. The concentration of the solute is determined online, via a high-performance liquid chromatography (HPLC) system with a diode array detector (g) (LaChrom L-7455) (Ashraf-Khorassani et al., 1997b). A fixed volume (25 μL) is removed and decompressed from the recirculation loop through a two-position six-way valve

Table 1. Solubility *S* of Naphthalene in Carbon Dioxide at 308 K and 328 K

308 K		328 K	
P (MPa)	*S* (10^{-2} mol/L)	*P* (MPa)	*S* (10^{-2} mol/L)
8.6	14.5	8.0	1.15
8.8	15.3	10.1	2.80
9.1	17.1	10.7	7.58
9.6	19.0	12.2	22.3
11.9	24.3	14.7	44.6
15.0	26.4	17.2	57.4
17.4	29.9	19.4	71.6
20.6	34.6	25.1	94.7
22.8	35.4	30.0	106
27.6	36.5		
30.1	39.0		

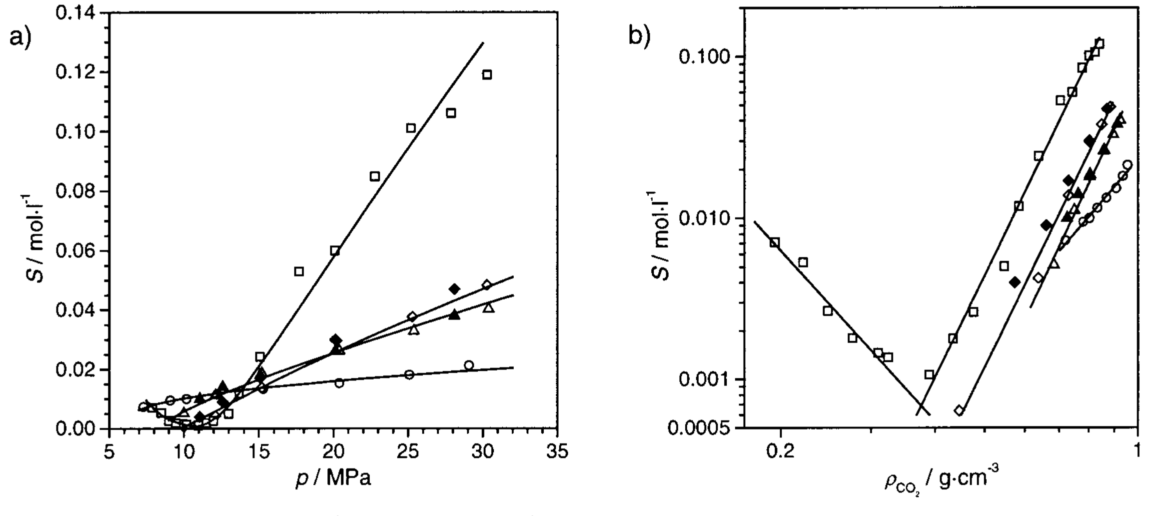

Figure 3. Solubility (a) and log−log plot of the solubility (b) of triphenylphosphine in carbon dioxide: this work, (○) 300 K, (△) 310 K, (◇) 320 K, and (□) 330 K; Schmitt and Reid (1988), (▲) 310 K, (◆) 320 K. Interpolations are from eq 1.

Table 2. Solubility *S* of Triphenylphosphine in Carbon Dioxide at 300 K, 310 K, 320 K, and 330 K

300 K		310 K		320 K		330 K	
P (MPa)	*S* (10^{-2} mol/L)	*P* (MPa)	*S* (10^{-2} mol/L)	*P* (MPa)	*S* (10^{-2} mol/L)	*P* (MPa)	*S* (10^{-2} mol/L)
7.3	0.728	10.0	0.516	10.0	0.064	7.9	0.712
9.1	0.947	12.1	1.12	12.1	0.426	8.5	0.534
10.2	0.997	15.2	1.86	15.2	1.38	9	0.266
12.2	1.15	20.4	2.62	20.2	2.96	9.5	0.181
15.3	1.33	25.4	3.29	25.3	3.77	10	0.146
20.4	1.52	30.4	4.04	30.3	4.84	10.2	0.137
25.1	1.81					11	0.107
29.1	2.12					11.5	0.179
						12	0.261
						13	0.503
						13.7	1.18
						15.1	2.42
						17.7	5.30
						20.1	6.00
						22.8	8.48
						25.2	10.1
						27.9	10.6
						30.3	11.9

Table 3. Solubility *S* of Tris(pentafluorophenyl)phosphine in Carbon Dioxide at 300 K, 310 K, and 320 K

300 K		310 K		320 K	
P (MPa)	*S* (10^{-2} mol/L)	*P* (MPa)	*S* (10^{-2} mol/L)	*P* (MPa)	*S* (10^{-2} mol/L)
6.9	10.3	8.2	0.47	10.0	1.58
7.2	13.8	8.3	0.92	10.1	2.42
7.4	15.0	8.4	1.64	10.2	3.36
7.9	15.3	8.5	2.40	10.3	3.90
8.0	16.8	8.7	6.95	10.5	5.52
8.2	16.5	8.8	9.93	10.6	6.42
8.6	17.9	8.9	11.3	10.7	8.80
8.8	19.9	9.0	13.2	10.8	12.8
9.0	18.7	9.2	17.4	10.9	15.0
9.5	22.0	9.5	22.8	11.0	22.1
10.3	21.5			11.1	24.6
11.0	24.0				
12.0	25.9				

Table 4. Solubility *S* of Tris(*p*-fluorophenyl)phosphine in Carbon Dioxide at 300 K, 310 K, and 320 K

300 K		310 K		320 K	
P (MPa)	*S* (10^{-2} mol/L)	*P* (MPa)	*S* (10^{-2} mol/L)	*P* (MPa)	*S* (10^{-2} mol/L)
7.0	5.8	8.5	0.85	10.0	0.44
7.3	7.3	8.7	1.65	10.5	1.09
7.6	8.5	8.9	2.41	11.1	1.87
7.9	10.0	9.1	3.23	11.6	3.25
8.3	11.3	9.3	3.77	12.1	4.57
8.7	12.7	9.6	4.84	12.6	6.05
9.0	14.3	10.1	6.0	13.0	7.48
9.5	15.8	10.6	7.9	13.4	8.1
10.0	17.2	11.1	9.5	14.0	9.3
10.6	18.5	11.6	10.9	15.1	13.1
11.0	20.2	12.2	12.9	15.5	15.5
		13.1	16.0	16.1	20.3
		14.0	18.3	16.5	18.2
		15.0	20.5	17.0	23.8
		16.0	23.0	17.5	25.5
		17.2	24.1	18.2	28.6
				18.6	32.9
				18.9	35.0

(c). Via a three-way valve (f), the excess gaseous CO_2 is removed from the sample loop ahead of the HPLC column (Vydac RPC_{18}, 14 cm). The remaining solute is rinsed out off the sampling loop onto the column at ambient temperature by acetonitrile as the mobile phase. After each measurement, the sampling loop (c) was cleaned with liquid CO_2 through valve (e) before switching it back in the recirculation loop. For a detailed description of the positions of the valves (c) and (e) in the experiments, see Ashraf-Khorassani et al. (1997). The HPLC system has been calibrated via an external six-way valve (h) (Valco 6UW) with a sampling loop of the same volume as (c). Errors in HPLC calibration are below 4%. As the pressure had to be increased during a series of measurements, the reproducibility and uncertainty of the experimental data were determined in the pressure range from 8.6 MPa to 9.1 MPa at 308.0 K with naphthalene. From eight concentrations, an average solubility of 0.160 mol/L with a standard deviation of 0.011 mol/L was calculated, which is equal to an error of 7% of the experimentally determined solubilities. Measurements are carried out over a temperature range from 300.0 K to 330.0 K and pressures up to 30 MPa.

Experimental Results and Discussion

Prior to the investigation of the phosphines, solubility measurements were performed with naphthalene (Table 1, Figure 2). The two isotherms at 308.0 K and 328.0 K agreed well with literature data (Tsekhanskaya et al., 1964;

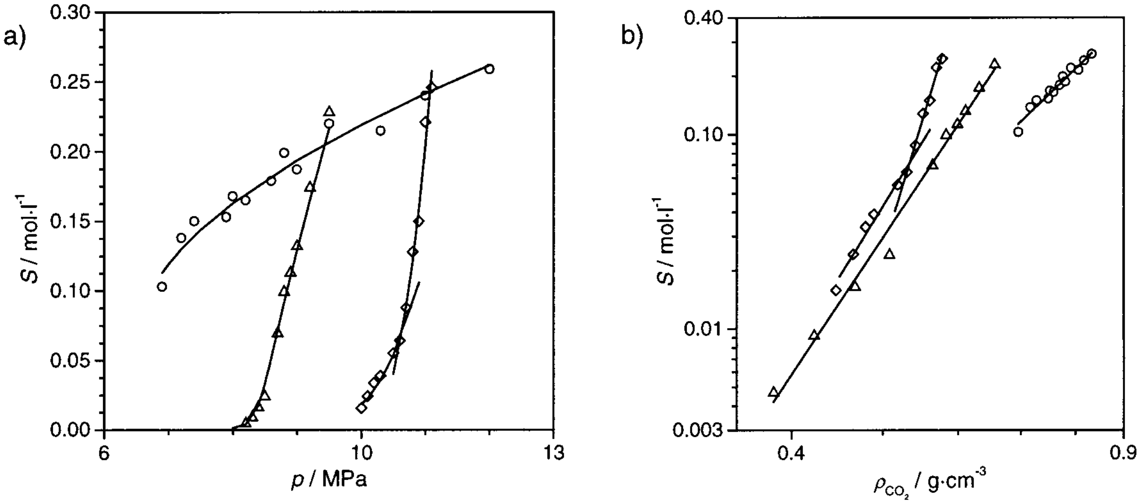

Figure 4. Solubility (a) and log–log plot of the solubility (b) of tris(pentafluorophenyl)phosphine in carbon dioxide at (○) 300 K, (△) 310 K, and (◇) 320 K. Interpolations are from eq 1.

Table 5. Solubility *S* of Tris(*p*-trifluoromethylphenyl)phosphine in Carbon Dioxide at 300 K, 310 K, and 320 K[a]

300 K		310 K		320 K	
P (MPa)	*S* (10^{-2} mol/L)	*P* (MPa)	*S* (10^{-2} mol/L)	*P* (MPa)	*S* (10^{-2} mol/L)
6.0	0.2	8.2	0.10	7.3	1.57
6.1	0.3	8.3	0.25	8.0	1.93
6.3	1.1	8.4	0.92	8.5	2.22
6.4	1.3	8.5	1.76	8.7	2.67
6.5	1.6	8.6	4.66	9.0	2.85
6.7	9.3	8.7	5.57	9.2	2.93
6.8	47.0	8.8	9.4	9.4	3.42
		8.9	11.7	9.7	3.6
		9.0	16.0	9.8	3.6
		9.1	19.9	9.9	4.2
		9.2	27.1	10.2	4.4
		9.3	41.4	10.4	4.4
				10.6	4.6
				10.8	4.6
				(11.0)	(5.3)
				(10.5)	(2.5)
				(10.6)	(3.5)
				(10.7)	(3.5)
				11.0	7.6
				11.2	9.6
				11.3	11.7
				11.3	12.1
				11.4	13.8
				11.5	16.2
				11.6	18.6
				11.7	24.4
				11.9	30.7
				12.0	35.1

[a] Solubilities at metastable state are in parentheses.

McHugh and Paulaitis, 1980; Liu and Nagahama, 1996).

Triphenylphosphine. In Figure 3a, the solubility of triphenylphosphine at 300.0 K, 310.0 K, 320.0 K, and 330.0 K is plotted versus pressure *p*. At 310.0 K and 320.0 K good agreement with available literature values (Schmitt and Reid, 1988) was found. The data are compiled in Table 2. The triphenylphosphine-rich phase remained solid over the whole investigated pressure range at the lower temperatures, whereas melting was observed in the region of minimum solubility at 330.0 K. The isotherms can be interpolated by the following function (Robin and Vodar, 1953; Stahl et al., 1978; Chrastil, 1982)

$$\ln(S_i/\mathrm{mol{\cdot}L^{-1}}) = a \ln\{\rho_{\mathrm{CO_2}}/(\mathrm{g{\cdot}cm^{-3}})\} + b \qquad (1)$$

In this equation, S_i is the solubility of the solute *i*, $\rho_{\mathrm{CO_2}}$ is the density of pure carbon dioxide, and *a* and *b* are temperature-dependent constants. Equation 1 also describes the measured solubilities well for the three other systems studied. The constants *a* and *b* are given in Table 6. Plotting ln *S* vs ln $\rho_{\mathrm{CO_2}}$ (Figure 3b) usually results in a group of parallel lines for the different temperatures. Only the isotherm at 300.0 K shows another slope *a*. As the slope of the interpolation function changes in the region of phase transition of triphenylphosphine at 330.0 K, the melting point is assumed to be at the intersection of both straight lines. By this method, the melting point is determined to be 330.0 K at 10.9 MPa, indicating that a solid–liquid–gas three-phase line was crossed (McHugh and Krukonis, 1986).

Tris(pentafluorophenyl)phosphine. The solubility of tris(pentafluorophenyl)phosphine was measured at three temperatures, 300.0 K, 310.0 K, and 320.0 K. The results are given in Table 3 and are displayed in Figure 4a. At 320.0 K, melting was observed in a pressure region from 8.5 to 9.0 MPa. At 300.0 K and 310.0 K, the solute was

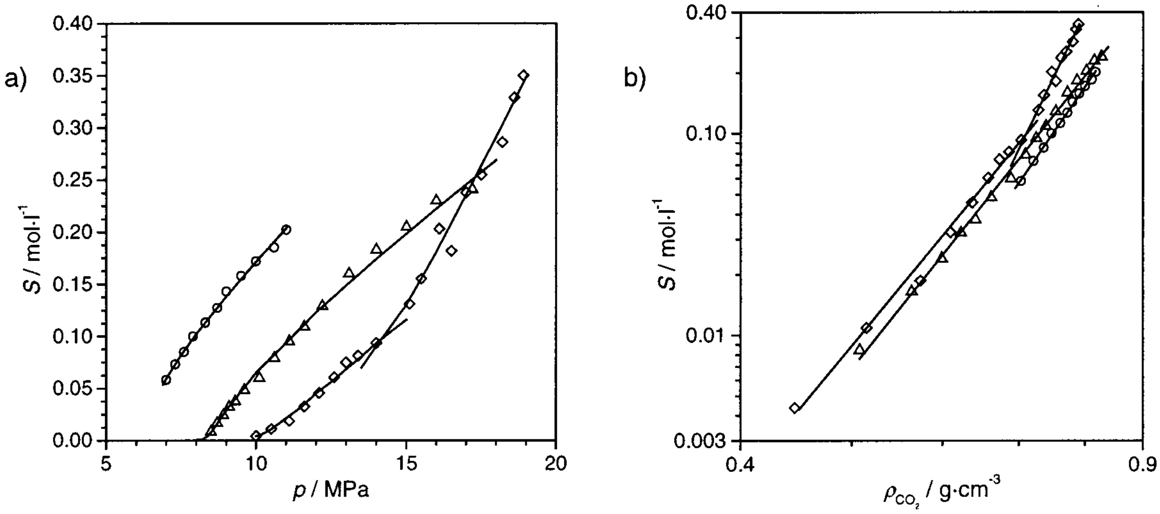

Figure 5. Solubility (a) and log−log plot of the solubility (b) of tris(*p*-fluorophenyl)phosphine in carbon dioxide at (○) 300 K, (△) 310 K, and (◇) 320 K. Interpolations are from eq 1.

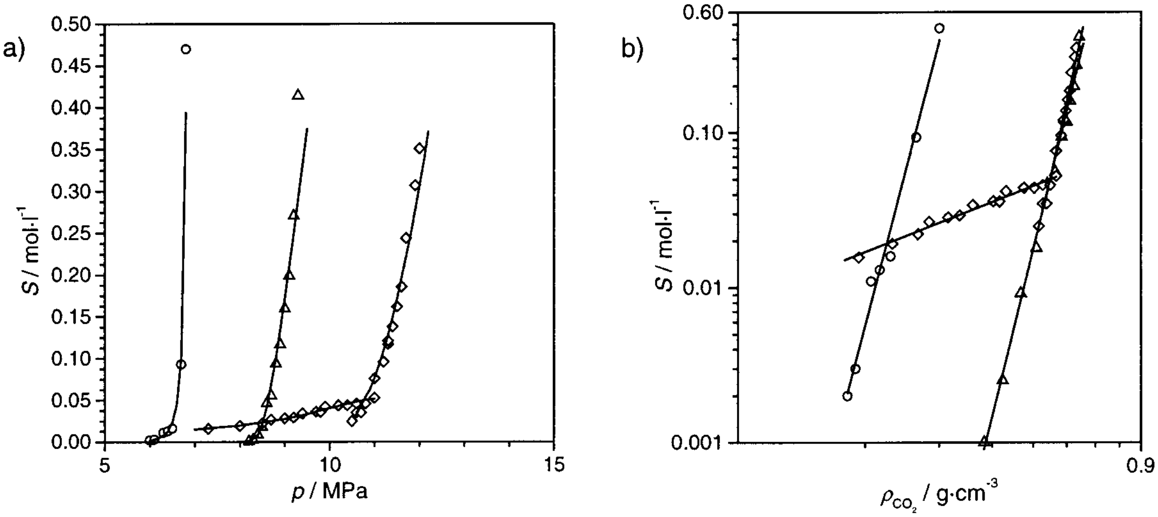

Figure 6. Solubility (a) and log−log plot of the solubility (b) of tris(*p*-trifluoromethylphenyl)phosphine in carbon dioxide at (○) 300 K, (△) 310 K, and (◇) 320 K. Interpolations are from eq 1.

Table 6. Parameters of the Interpolation Function Eq 1

component	*T*/K	*a*	*b*
naphthalene	308	2.515	−0.762
$C_{10}H_8$	328	3.364	0.605
triphenylphosphine	300	3.667	−3.772
$P(C_6H_5)_3$	310	6.725	−2.629
	320	6.502	−2.236
	330	−3.444	−10.591 (<10.9 MPa)
		6.553	−0.900 (>10.9 MPa)
tris(pentafluorophenyl)phosphine	300	4.664	−0.480
$P(C_6F_5)_3$	310	7.359	1.574
	320	7.995	2.363 (<10.7 MPa)
		16.076	7.475 (>10.7 MPa)
tris(*p*-fluorophenyl)phosphine	300	8.180	0.058
$P(C_6H_4F)_3$	310	7.097	−0.060
	320	6.900	0.049 (<14.3 MPa)
		11.795	1.731 (>14.3 MPa)
tris(*p*-trifluoromethylphenyl)phosphine	300	10.456	11.629
$P[4\text{-}(CF_3)C_6H_4]_3$	310	11.222	3.752
	320	1.065	−2.356 (<10.8 MPa)
		12.673	4.673 (>10.8 MPa)

solid at all pressures. Although no phase transition could be detected visually, in the log−log-plot of solubility vs density of CO_2 (Figure 4b), there is a change in the slope *a* of the interpolation function at 320.0 K. This could indicate the existence of a second three-phase line at 320.0 K and 0.537 g/cm^3 or 10.7 MPa, which causes the transition between two different liquid phases. Unfortunately, limited by the experimental setup, we were not able to differentiate between the existence of one or more interfaces between the corresponding two or more fluid phases. Therefore, we could not observe the presence of a liquid−liquid−gas three-phase line. For this purpose, a second window for a view from the side is planned.

Tris(p-fluorophenyl)phosphine. In Figure 5a and Table 4, the solubility isotherms of tris(*p*-fluorophenyl)phosphine are presented. At all three temperatures, melting was observed: at 300.0 K in a region around 7.5 MPa, at 310.0 K around 6.1 MPa, and at 320.0 K at 5.4 MPa. The decreasing melting pressures with rising temperature indicate a three-phase line with a negative slope in a p,T projection. Because of experimental limitations, caused by the relatively low density of carbon dioxide and low concentration of the solute, data could not be recorded in the melting region. As can be seen in Figure 5b, at 320.0 K a change in the slope a of the interpolation function was found at 14.3 MPa. In this pressure region, the liquid tris(*p*-fluorophenyl)phosphine rich phase became cloudy, but solidification could not be observed.

Tris(p-trifluoromethylphenyl)phosphine. Melting was observed at all temperatures: at 300.0 K below 2.5 MPa, at 310.0 K below 2.0 MPa, and at 320.0 K at even lower pressure. A change in the slope a, which could correspond to a liquid−liquid transition point, was observed at 320.0 K and 10.8 MPa. Remarkable is the steep increase of the 300.0 K isotherm below 7.0 MPa, resulting in high solubilities at comparable low densities. The data are compiled in Figure 6 and in Table 5.

Conclusion

As expected, fluorination increases the solubility dramatically. Substitution of only one hydrogen atom by fluorine in the para position leads to an increase of solubility by about an order of magnitude (see tris(*p*-fluorophenyl)phosphine compared to triphenylphosphine). Perfluorination results in a further increase in solubility but to a markedly smaller extent. A further enhancement of the solubility is achieved by substitution of the fluorine atoms in tris(*p*-fluorophenyl)phosphine by CF_3 groups. So the solubility of the ligands can be controlled not only by the degree of fluorination but also by the position of fluorine atoms or fluorine-containing groups. In addition, the fluorination of the ligand is important with respect to the coordination ability of the resulting complexes and the catalysis of a reaction. To study these influences and the principle effect of fluorination on the phenomenology of the phase diagram, additional substances have to be investigated.

Acknowledgment

We gratefully acknowledge S. Verewkin for the very helpful discussions on phase equilibrium phenomena and Professor G. Kabo from the Belarus State University, Minsk.

Literature Cited

Ashraf-Khorassani, M.; Combs, M.; Taylor, L. Supercritical fluid extraction of metal ions and metal chelates from different environments *J. Chromatogr., A* **1997**, *774*, 37−49.

Ashraf-Khorassani, M.; Combs, M.; Taylor, L. Solubility of Metal Chelates and Their Extraction from an Aqueous Environment via Supercritical CO_2. *Talanta* **1997**, *44*, 755−763.

Chrastil, J. Solubility of Solids and Liquids in Supercritical Gases. *J. Phys. Chem.* **1982**, *86*, 3016−3021.

Dardin, A.; DeSimone, J. M.; Samulski, E. T. Fluorocarbons Dissolved in Supercritical Carbon Dioxide. NMR Evidence for Specific Solute−Solvent Interactions. *J. Phys. Chem. B* **1998**, *102*, 1775−1780.

Kainz, S.; Koch, D.; Baumann, W.; Leitner, W. Perfluoralkylsubstituierte Arylphosphane als Liganden für die homogene Katalyse in überkritischem Kohlendioxid. *Angew. Chem.* **1997**, *109*, 1699−1701.

Kazarian, S. G.; Vincent, M. F.; Bright, F. V.; Liotta, C. L.; Eckert, C. A. Specific Intermolecular Interaction of Carbon Dioxide with Polymers. *J. Am. Chem. Soc.* **1996**, *118*, 1729−1736.

Kreher, U.; Schebesta, S.; Walther, D. Übergangsmetall-Organoverbindungen in superkritischem Kohlendioxid: Löslichkeiten, Reaktionen, Katalysatoren. *Z. Anorg. Allg. Chem.* **1998**, *624*, 602−612.

Liu, G.; Nagahama, K. Solubility of Organic Solid Mixture in Supercritical Fluids. *J. Supercrit. Fluids* **1996**, *9*, 152−160.

Luks, K. D.; Kohn, J. P. The Topography of Multiphase Equilibria Behavior: What Can it Tell the Design Engineer. *Proceedings of the 63rd Annual Convention of the Gas Proccessors Association, New Orleans*; Gas Processors Association, Tulsa, OK, 1984; pp 181−186.

McHugh, M.; Krukonis, V. *Supercritical Fluid Extraction*: *Principles and Practice*; Butterworth: Stoneham, 1986.

McHugh, M.; Paulaitis, M. Solid Solubilities of Naphthalene and Biphenyl in Supercritical Carbon Dioxide. *J. Chem. Eng. Data* **1980**, *25*, 326−329.

Morita, D. K.; Pesiri, D. R.; David, S. A.; Glaze, W. H.; Tumas, W. Palladium-Catalyzed Cross-Coupling Reactions in Supercritical Carbon Dioxide. *Chem. Commun.* (*Cambridge*) **1998** 1397−1398.

Palo, D. R.; Erkey, C. Homogeneous Catalytic Hydroformylation of 1-Octene in Supercritical Carbon Dioxide Using a Novel Rhodium Catalyst with Fluorinated Arylphosphine Ligands. *Ind. Eng. Chem. Res.* **1998**, *37*, 4203−4206.

Peters, C. Multiphase Equilibria In Near-Critical Solvents, In *Supercritical Fluids, Fundamentals and Applications*; Kiran, E., Levelt Sengers, J., Eds.; NATO ASI Series, Series E: Applied Sciences; Kluwer: Dordrecht, 1994; Vol. 273, pp 117−145.

Peters, C. J.; de Roo, J. L.; de Swaan Arons, J. Phase equilibria in binary mixtures of propane and triphenylmethane. *Fluid Phase Equilib.* **1995**, *109*, 99−111.

Robin, S.; Vodar, B. Solubility in Compressed Gases. *Discuss. Faraday Soc.* **1953**, 233−238

Schmitt, W.; Reid, R. The Solubility of Parafinic Hydrocarbons and Their Derivates in Supercritical Carbon Dioxide. *Chem. Eng. Commun.* **1988**, *64*, 155−176.

Smart, N.; Carleson, T.; Kast, T.; Clifford, A.; Burford, M.; Wai, C. Solubility of Chelating Agents and Metal-Containing Compounds in Supercritical Fluid Carbon Dioxide. *Talanta* **1997**, *44*, 137−150

Stahl, E.; Schilz, W.; Schütz, E.; Willing, E. A Quick Method for the Microanalytical Evaluation of the Dissolving Power of Supercritical Gases. *Angew. Chem., Int. Ed. Engl.* **1978**, *17*, 731−738

Stradi, B.; Kohn, J.; Stadtherr, M.; Brennecke, J. Phase Behavior of the Reactants, Products and Catalysts Involved in the Allylic Epoxidation of *trans*-2-Hexen-1-ol to (2R,3R)−(+)-3-Propyloxiranemethanol in High-Pressure Carbon Dioxide. *J. Supercrit. Fluids* **1998**, *12*, 109−122.

Tsekhanskaya, Y.; Iomtev, M.; Mushkina, E. Solubility of Naphthalene in Ethylene and Carbon Dioxide under Pressure. *Russ. J. Phys. Chem.* **1964**, *38*, 1173−1176.

Wai, C. M.; Wang, S. Supercritical Fluid Extraction: Metals as Complexes *J. Chromatogr., A* **1997**, *785*, 369−383.

Yazdi, A. V.; Beckman, E. J. Design, Synthesis and Evaluation of Novel, Highly CO_2-Soluble Chelating Agents for Removal of Metals. *Ind. Eng. Chem. Res.* **1996**, *35*, 3644−3652.

Yee, G.; Fulton, J.; Smith, R. Fourier Transform Infrared Spectroscopy of Molecular Interactions of Heptafluoro-1-butanol or 1-Butanol in Supercritical Carbon Dioxide and Supercritical Ethane. *J. Phys. Chem.* **1992**, *96*, 6172−6181

Received for review November 4, 1999. Accepted April 14, 2000.

JE9902995